SEISMOTECTONICS OF DELHI REGION

by R. K. S. CHOUHAN, *Department of Applied Geophysics, Indian School of Mines, Dhanbad-826004*

(Communicated by Prof. S. N. Sarkar, F.N.A.)

(Received 24 September 1974; after revision 1 July 1975)

An attempt has been made to study the seismotectonics of the Delhi region. It is observed that the trijunction of the Delhi-Hardwar ridge, Lahore-Delhi ridge and the Delhi axis of folding is most active seismically; generating shocks having focal depths of about 8 km. Space and time distribution of strain has been studied by using earthquake data of 11 years. Frequency magnitude analysis has been carried out for earthquakes having $M \geqslant 2$. The focal mechanism solutions show that the Kumaon area is under compression while the Delhi area is under tension.

INTRODUCTION

The area around Delhi has been experiencing a series of earthquakes of mild intensity since 1963. These were in general followed by thundering sound and many of them were felt at Rohtak, Sonepat, Delhi, Gurgaon, Meerut and close to Panipat. These minor shocks have been studied by Hukku (1964, 1966), Singh (1964), Sharma (1965), Srivastava and Somayajulu (1966), and Tandon and Chaudhury (1966). Most of these shocks are interpreted to be of shallow focus with epicentres, in most cases, located west of Delhi and the concentration of the epicentre being around Sonepat, Rohtak and close to Gurgaon.

Various theories have been put forward to explain the causes of these earthquakes:—

(*a*) Singh (1964) attributes these shocks to waterlogging as a result of which the sandy beds did not permit the subsoil vapour to pass out and cause eruptions in the superficial layers leading to frequent tremors.

(*b*) Hukku (1966) attributes these shocks, which are felt locally, to collapse of limestone cavern that may exist along fault zones in the Vindhyan limestones covering the basement rocks. Hukku also postulates that the earthquakes around Delhi are probably related to the renewal of activity along suspected radial tear faults which may cut through the Aravalli basement and the overlying Vindhyan formations.

(*c*) Srivastava and Somayajulu (1966) consider that the tight wedging of the blocks along dislocations converging towards Delhi are mainly responsible for the earthquakes around Delhi.

The seismicity around Delhi has not started abruptly. The seismic history of the area can be traced as far back as 1720. However, the microtremors were recorded only after 1962 when short period high magnification seismographs were installed at

Delhi seismological observatory. Important earthquakes occurred around Delhi are as follows :—

TABLE I

Important earthquakes that occurred around Delhi

Magnitude values preceeding (A) are approximate values determined from macroseismic data.

S. No.	Date	Location	Magnitude M	Remarks
1.	1720–July 15	Probably near Delhi.	6.5 (A)	Maximum observed intensity on MM scale was IX.
2.	1764–June 4	Banks of Ganges	6.0 (A)	Maximum observed intensity on MM Scale was IX.
3.	1803–Sept. 1	Near Mathura	6.5 (A)	Maximum observed intensity on MM Scale was IX.
4.	1842–March 5	Near Mussourie	5.5 (A)	Maximum intensity on MM scale was VII.
5.	1848–April 26	Mt. Abu	6.0 (A)	Maximum intensity on MM scale was VII.
6.	1852 -March 31	Near Meerut	—	—
7.	1906–Aug. 15	Near Mt. Abu	5.0	—
8.	1911–Oct. 14	31°N, 80.5°E	6.75	—
9.	1916–Aug. 28	30°N, 81.0°E	7.5	—
10.	1934–April 14	29°N, 75.5°E	5.0	—
11.	1935–March 6	29.45°N, 80.15°E	6.0	—
12.	1937–Oct. 20	31°N, 78°E	6.0 (A)	Maximum observed intensity on MM Scale was VII.
13.	1956– Oct. 10	28.15°N, 77.67°E (Khurja)	6.7	Maximum observed intensity on MM Scale was VII with elliptical isoseismal running in E–W direction. The epicentral tract was about 20 Km (Jhingran & Puri 1963).
14.	1958–Dec. 28	30°N, 80°E	6.3	—
15.	1960–Aug. 27	28.2°W, 77.4°N (Gurgaon)	6.0	Major axis of the ellipse enclosing the maximum recorded intensity VII extended for a length of about 35 km runs, in a NNE–SSW direction (Muktinath *et al.* 1960).
16.	1964–Oct. 3	Near Sonepat	—	The maximum recorded intensity on MM scale was V and the isoseismal was elliptical in nature with the major axis running in N–S direction.
17.	1966–Aug. 15	28.67°N, 78.93°E	5.3	—
18.	1969–June 22	30.0°N, 79.3°E	5.8	—
19.	1971–Jan. 27	Rohtak	5.3	—

(—) Data Not Available.

The objective of this paper is to study the seismotectonics of a transverse section of the Himalayas with emphasis on the Delhi region. To accomplish this the earthquake data of I.M.D. from 1962 to 1972 has been used along with other important earthquakes of the area (Table I).

Tectonic History

Agocs (1956), Bose (1957), Ghosh (1959), and Simha (1959) carried out geophysical work in this area and suggested the presence of a number of faults. Krishnaswamy (1962) also concluded from a study of basement contours the presence of a few tear faults.

The area around Delhi is mostly covered by alluvium. Outcrops of Alwar quartzites are observed in Delhi and the area lying southwards. The quartzites are, in general, highly jointed and folded. The hot spring at Sohna in Gurgaon district is observed to emanate close to a N-S trending fault scarp (Hukku 1966).

Tectonic map of India has been prepared by the scientists of Oil and Natural Gas Commission (ONGC). According to Negi and Ermenko (1968) following is a brief description of the tectonics of the area.

The tectonic evolution of the platform started with the development of several major super order and first order structures with the deposition of Cuddapah sequence (Proterozoic). Probably, Delhi orogenic cycle may be proterozoic.

Extensive area of the Indian platform underwent subsidence during this period (upper Proterozoic to lower Palaeozoic) to give rise to different super order and first order structures. The Cuddapah and the Vindhyan systems, wherever they occur together, are separated by a period of intense tectonic activity resulting in major change in the pre-existing structural pattern. The Vindhyan is much less disturbed, practically, devoid of metamorphism with less frequent basic intrusives. The sequence shows extensive development to the north of Narmada fault zone in the Vindhyan synclines, west Uttar Pradesh and east Uttar Pradesh shelves, and in the Rajasthan shelf.

The Palaeogene marks, the tectonic evolution of Mesozoic and Palaeogene sequences were frequently faulted. The Punjab shelf originated during this stage. The west and east Uttar Pradesh shelves, which probably completed the first phase of tectonic evolution during the Vindhyan, underwent final phase of evolution during this time. All these tectonic units of the Delhi region including the frontal folded zone of the Himalayas are shown in Fig. 1. (after Negi & Ermenko 1968). The following tectonic units can be recognised :

(*i*) Frontal folded zone, (*ii*) Areas of Delhi folding, (*iii*) Rajasthan shelf, (*iv*) Lahore Delhi ridge, (*v*) Punjab shelf, (*vi*) Delhi-Hardwar ridge, (*vii*) West Uttar Pradesh shelf and (*viii*) Sarda depression.

Seismicity

Fig. 1 also shows all epicentres of the recorded earthquakes having magnitude $M \geqslant 2$. Numbers above the epicentres refer to number of shocks from the same source. From this seismotectonic map it appears that the most active area is the junction of the Delhi-Hardwar ridge, the Lahore-Delhi ridge and the axis of Delhi

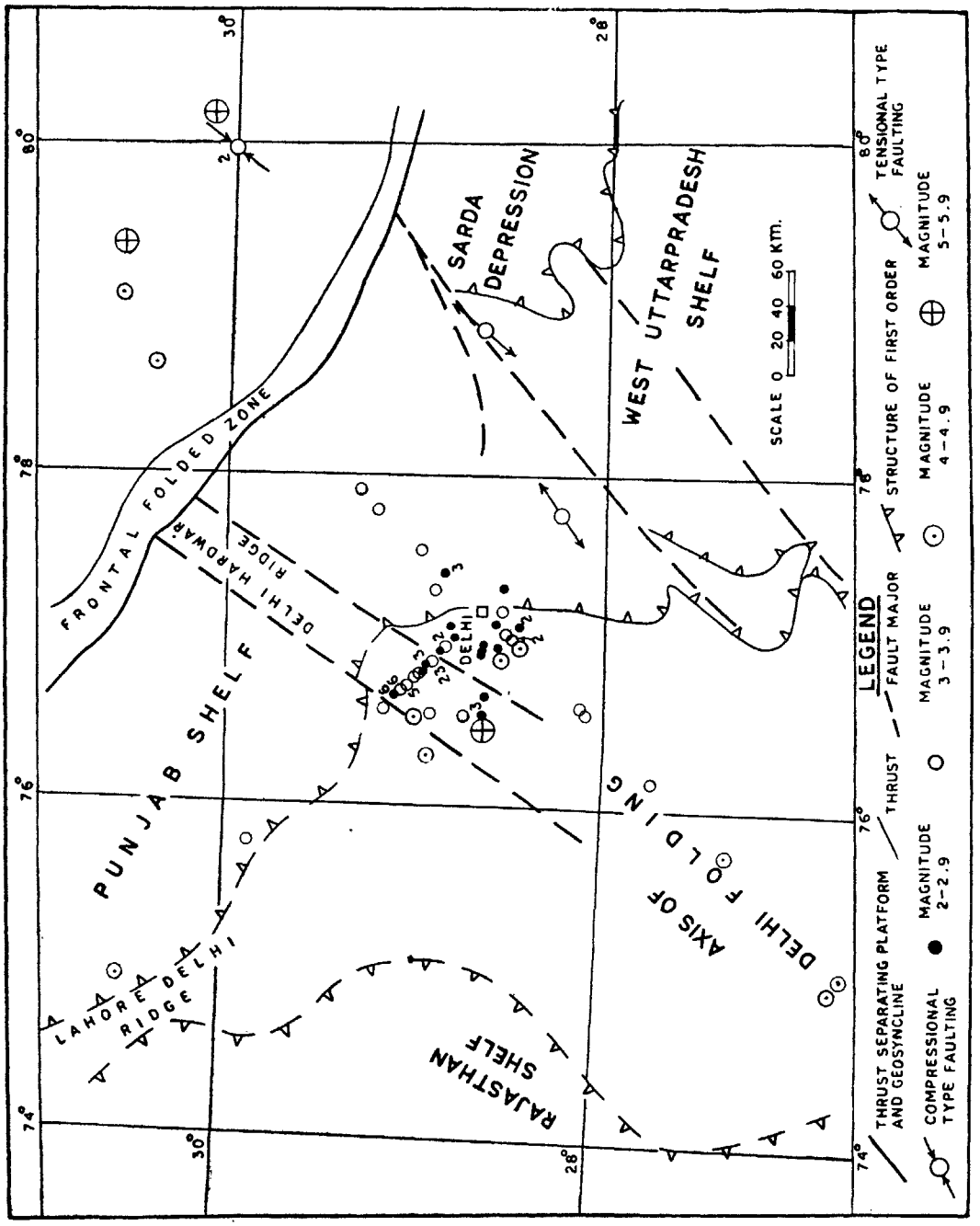

FIG. 1. Tectonic map of the Delhi region and surrounding area after Negi and Ermenko (1968) and the epicentres of earthquakes having $M \geq 2$, the numbers following the epicentres being the number of shocks from the same source. The figure also shows the focal mechanism solutions of the Delhi earthquake (tensional type) and the Kumaon earthquakes (pressure type).

folding as maximum concentration of earthquakes occur in this area. Second active zone is the axis of Delhi foldings which extends in the same direction beyond Delhi in a linear fashion (NE-SW direction). A few moderate shocks are found to occur along the Moradabad fault. This figure also shows three epicentres (two in Delhi region and one in Kumaon) whose focal mechanism solutions have been studied, along with the direction of maximum tension (for the Delhi region) and maximum pressure (for the Kumaon region) as derived in the present study (to be given later).

Focal Coordinates

The focal depth of a shallow earthquake which has its focus in the earth's crust is generally determined with reasonable precision if the epicentral distance of at least one seismographic station does not exceed the depth of focus. The travel time curve of the wave which travels directly from the focus to the recording stations is very nearly a straight line except for the portion close to the epicentre. In such a travel time curve if $\triangle$ is the epicentral distance, and t, the travel time of the direct wave then

$$t = d/v = \frac{\sqrt{\triangle^2 + h^2}}{v} \quad \ldots \quad (1)$$

where d is the focal distance, h, the depth of focus, and v, the speed in the upper layer of the earth's crust (Average Velocity).

If $\triangle$ is large with respect to h, then (1) is closely approximated by $t = \triangle/v$ which corresponds to the linear portion of the travel time curve. The extrapolation of the straight line to cut the time axis will give the time of occurrence of the earthquake.

From (1) we get $h = \sqrt{d^2 - \triangle^2}$, ... (2)

Let us see the effect on h of an uncertainty in $\triangle$ from

$$\left|\frac{\partial h}{\partial \triangle}\right| = \frac{\triangle}{\sqrt{d^2 - \triangle^2}} = \frac{\triangle}{h} \quad \ldots \quad (3)$$

That is, for a shock 10 km (h) deep, an uncertainty of 2 km ($\partial\triangle$) in the epicentre location would introduce an uncertainty of 10 km (∂h) in the computed value of h if the nearest station were 50 km ($\triangle$) from the epicenter, but, an uncertainty of only 2 km (∂h) if the nearest station were 10 km ($\triangle$).

Generally, P_g and S_g waves can be identified from the seismograms of the tremors originating around Delhi. All these records are due to local earthquakes and since we have limited observatories around Delhi it is not possible to have more than a few records of each tremor. As an alternative, a critical study of the arrival times of P_g and S_g suggests that the focal depths are very small (a few km) in most of the cases except a few, where the focal depth may be slightly higher. Hence for the present purpose, it has been assumed that the focal depth of all the tremors are nearly the same. Thus, we get records of P_g and S_g at different epicentral distances for various tremors. Using the following procedure, the focal depth has been determined for earthquakes around Delhi.

Origin time 't_o' is determined from the relation after Tocher (1959)

$$t_o = t_{P_g} - \frac{t_{S_g} - t_{P_g}}{0.732} = t_{P_g} - t \quad \ldots \quad (4)$$

where t_{P_g} is the arrival time of the direct P_g wave and t_{S_g} arrival time of direct S_g wave. The divisor 0.732 comes from classical elastic theory and depends on the following assumptions :

(1) The P_g and S_g waves originate at the same time and place.

(2) Poisson's condition is satisfied in the rock between the focus and the recording station.

Using relation (4) the travel times for P_g waves have been computed from the selected earthquake data of the Delhi region for the year 1964 (Table II).

$T - \triangle$ curve has been plotted from the data of Table II in Fig. 2. The nature of the curve, as defined by equation (1), is a hyperbola which can be written as

$$t^2v^2 - \triangle^2 = h^2 \qquad \ldots \quad (5)$$

Now, we need simply to locate the point at which $\triangle = 0$, i.e., the travel time of P_g wave from the focus to the epicentre, and, therefore, for this point (5) becomes

$$t^2v^2 = h^2 \text{ or } h = tv \qquad \ldots \quad (6)$$

TABLE II

Date	Arrival time of P_g			Arrival time of S_g			in kms	T Travel time of P_g in secs.	$t_{S_g} - t_{P_g}$ in secs.
	H	M	S	H	M	S			
6-1-64	19	20	17.3	19	20	23.5	56	8.6	6.2
6-1-64	16	15	05.5	16	15	09.5	30	5.5	4.0
9-1-64	06	46	46.5	06	46	50.2	30	5.0	3.7
16-1-64	19	01	39.0	19	01	43.6	40	6.2	4.6
2-2-64	00	00	09.0	00	00	11.0	20	2.9	2.0
2-2-64	01	17	03.7	01	17	06.9	30	4.4	3.2
10-2-64	17	11	45.0	17	11	56.7	100	16.1	11.7
4-3-64	18	00	18.2	18	00	20.2	17	2.9	2.0
24-3-64	17	52	12.2	17	52	16.7	40	6.1	4.5
24-4-64	07	54	12.0	07	54	14.0	20	2.9	2.0
29-4-64	01	59	22.2	01	59	23.7	10	2.0	1.5
28-5-64	16	14	29.2	16	14	30.6	10	1.9	1.4
28-5-64	21	56	38.4	21	56	43.7	45	6.9	5.3
1-8-64	16	23	28.5	16	23	34.0	47	7.5	5.5
10-8-64	12	11	21.0	12	11	25.5	39	6.1	4.5
12-8-64	04	07	40.8	04	07	44.8	30	5.5	4.0
16-8-64	03	29	39.2	03	39	44.2	40	6.7	5.5
15-9-64	09	17	41.5	09	17	45.5	30	5.5	4.0
18-9-64	21	20	04.0	21	20	07.9	30	5.3	3.9
25-9-64	07	45	02.4	07	45	04.1	15	2.5	1.7
28-9-64	06	49	41.6	06	49	45.2	30	4.9	3.6
29-10-64	14	29	02.0	14	29	06.0	40	5.5	4.0
06-11-64	02	25	53.5	02	26	01.5	70	11.0	8.0

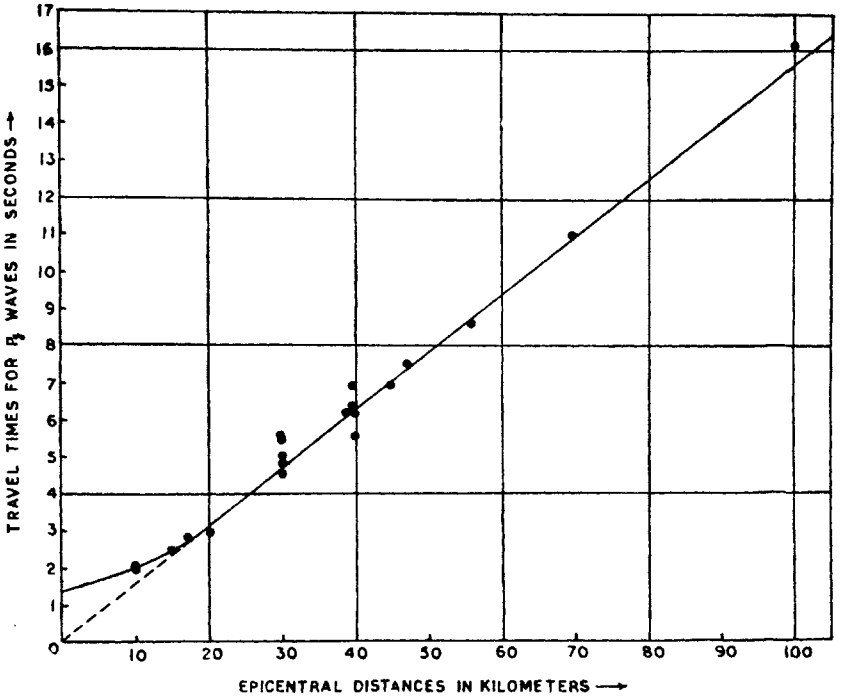

FIG. 2. Travel time curve for P_g wave.

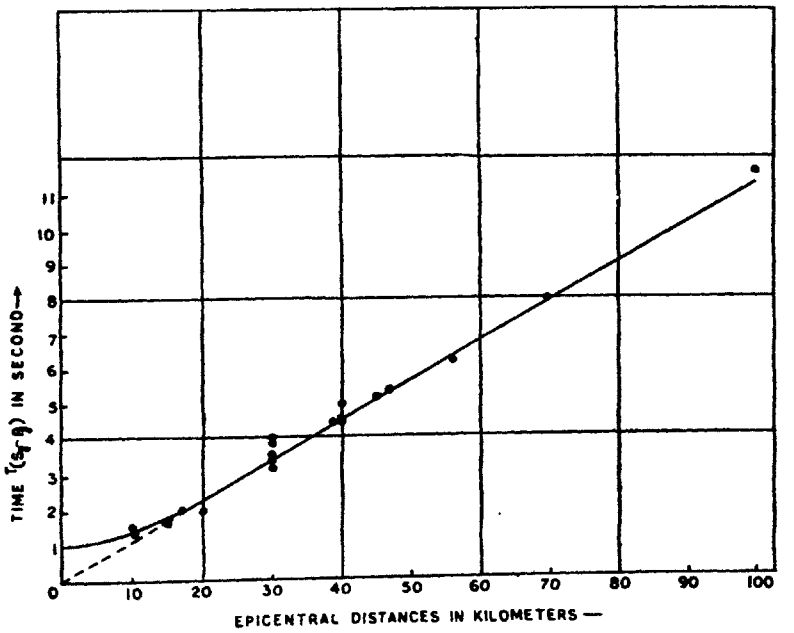

FIG. 3. Showing $T(S_g, P_g)$ against epicentral distance.

Hence, h, the depth of focus can be calculated from the intercept of the curve on the time axis (Fig. 2) and the velocity can be calculated from the same curve by taking $d\triangle/dt$ of the linear segment. For the present case, $t = 1.35$ seconds and $v = 5.8$ km/sec., the velocity of P_g wave, the focal depth comes to be 7.9 km.

This focal depth can also be obtained from Fig. 3 by plotting the time $(ts_g - tp_g)$ against the epicentral distance and making the same assumptions as in the above method. In addition, it is also assumed that the focus lies within the granitic layer. Here also a similar curve is obtained but the point where the curve intersects the time axis gives the time of separation of P_g and S_g waves at the epicentre. But this value is zero at the focus because of assumption (2). Hence to calculate the focal depth, it is necessary to find out the rate of separation of the time $(ts_g - tp_g)$ with the epicentral distance, i.e., $d\triangle/d(ts_g - tp_g)$ which can be determined from Fig. 3. The value of $(ts_g - tp_g)$ at the epicentre is 1 second and $d\triangle/d(ts_g - tp_g)$ is 8.1 km/sec. Hence, the focal depth becomes 8.1 km; a value very close to that obtained by the first method.

Frequency-Magnitude Analysis

The distribution of earthquakes magnitude versus frequency has been expressed by Gütenberg and Richter (1954) as

$$\log N = a - bM, \qquad \ldots \quad (7)$$

where N is the number of earthquakes with magnitude between M and $M + dM$ and 'a' and 'b' are constants. This equation has been largely used by many seismologists notably Isacks and Oliver (1964), Page (1968), Utsu (1971), Drakopoulos and Srivastava (1972), and Chouhan (1968, 1970).

In general the constants a and b have been determined by least square method. Since Utsu (1965) has proposed the maximum likelihood method, of estimating the value of b in the above relation, which is widely used at present has been used in the present analysis also. According to Utsu's (1965) method, the value of b can be estimated from the relation

$$b = \frac{0.4343}{(M_{aver} - M_{min})} \qquad \ldots \quad (8)$$

where M_{aver} is the average value of M and M_{min} is the lowest magnitude in the population. Relation (8) gives lower value of b if $\triangle M$ (magnitude interval) is greater than 0.25 and correct value can be restored by multiplying b with n, a function of $b.\triangle M$ (Utsu 1967).

In the present analysis there are 74 earthquakes with well defined magnitude $M \geqslant 2$ and remaining 92 with $M < 2$. Hence earthquake recurrence curve has been plotted using 74 earthquakes having $M \geqslant 2$ as shown in Fig. 4 from which the relation

$$\text{Log } N = 1.53 - 0.33\, M \qquad \ldots \quad (9)$$

has been obtained.

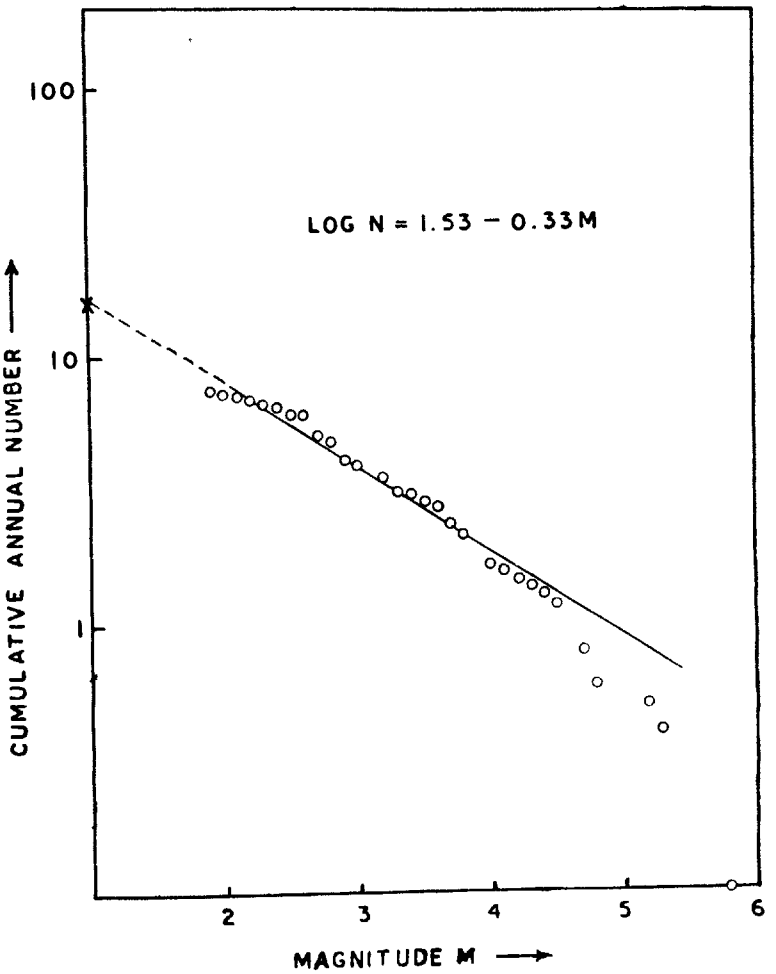

FIG. 4. Earthquake recurrence graph for M ⩾ 2. Cross mark on the figure shows the total number of recorded earthquakes per annum having M ⩾ 1.

The confidence limits for b value in this case is ± 0.08 which is fairly high demonstrating the reliability of the data used.

From equation (9), the ratio a/b can be determined which gives the magnitude of earthquake that may occur once in a year, i.e., when $n = 1$. This quantity has been used as a measure of seismicity (see Appendix I) by the author (1968, 1970). Similar results have also been reported by Utsu (1971) and Galanopoulos (1972). For the Delhi region this magnitude once per year is 4.7. In a similar way, the maximum size of an earthquake that may occur in this region appears to be 7.6. Tandon and Chaudhury (1966) have given a table for the return periods of earthquakes with magnitudes 5, 6 and 7 as 7, 25, and 100 years respectively.

Focal Mechanisms

An equal angle projection of the lower hemisphere of the focal sphere using Wullfnet has been used to study the focal mechanisms of the Delhi and Kumaon earthquakes. Values of '*i*', the angle of incidence at the source as measured from the downward vertical for a given distance are computed from the tables of Hodgson and Storey (1953). Similar method has been employed by Ritsema (1955) using Wullfnet and by Sykes (1967) using Schmidtnet. First motion *P* wave data for the present study has been taken from the International Seismological Summary and International Seismological Centre and some of the first motion data has been checked by the author from the traces of available seismograms. Table III shows a list of earthquakes used in this study. Fig. 5 shows a plot of '*i*' and the azimuth of the station with respect to the epicentre. In this figure, solid circles denote compressions, open circles denote dilatations, and the lines separating compressions and dilatations are nodal lines.

Table III

Earthquakes used for this study

Event	Date	Origin time			Latitude	Longitude	*M*
		H	M	S	N	E	
1.	October 10, '56	15	31	36.0	28.15°	77.67°	6.7
2.	August 15, '66	02	15	33.8	28.67°	78.93°	5.3
3.	December, 12 '58	05	34	38.0	30.01°	79.94°	6.3

(*a*) *The Delhi region:* Fig. 5 shows the focal mechanism solutions (events 1 and 2) of the Delhi region. The distribution of compressions and dilatations, as shown in the figure, suggests small normal components of faulting, the fault being of tensional type. The ratio of the strike slip to normal slip is about 1.5:1. Both the solutions show two steeply dipping nodal planes; one running in the east-west direction and the other in the north-south. The nodal planes of the event number 2 are uniquely defined whereas, for the event number 1, the planes have been drawn taking into account the solution of the event No. 2 and the distribution pattern of compressions and dilatations. The nodal planes drawn for the event No. 1 by the above procedure is justified because of sparse data and proximity of the solution. However, the nature of the solution will remain same, though the dip and strike of the nodal planes may change. In the present case the east-west nodal plane is taken as the fault plane and it represents a movement of right lateral strike slip motion. This nodal plane has been chosen as the fault plane because the major axis of the isoseismal lies approximately in the east-west direction (Jhingran & Puri 1963; and Tandon & Chaudhury 1966). The proximity of these two solutions may indicate that they are related to the same fault, in this case it may be the Moradadad fault. The maximum tension (*T*) axes for both the events are shown in Fig. 1 which are almost parallel to the Moradabad fault.

(*b*) *The Kumaon region:* The earthquake(event No. 3) which occurred in this region shows typical thrust faulting with steeply dipping nodal planes (Fig. 5). The nodal

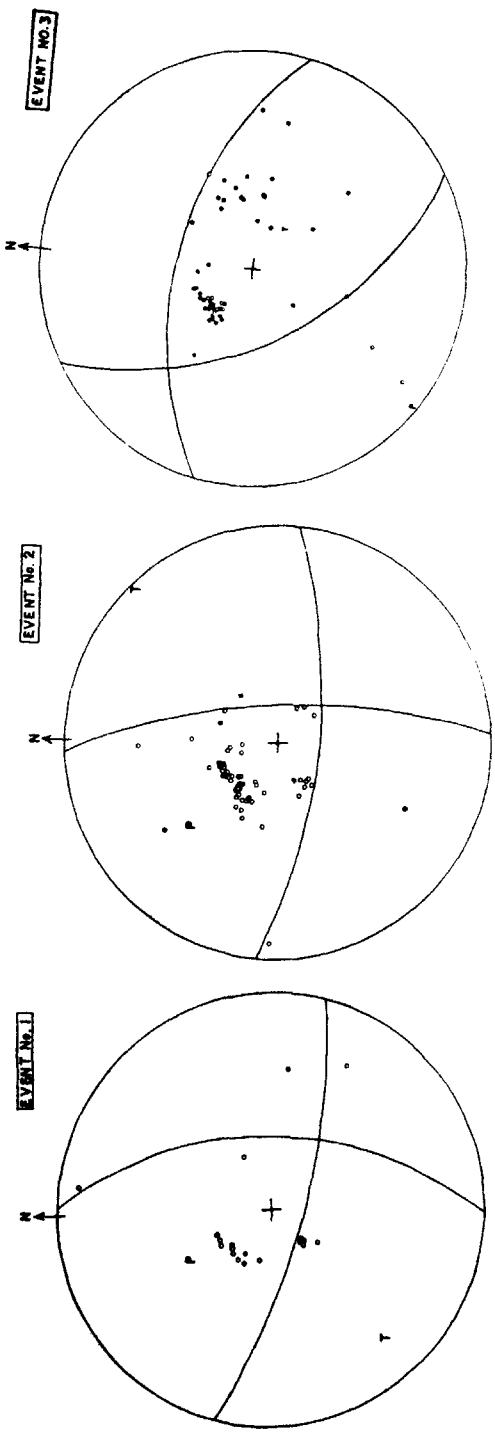

FIG. 5. Focal mechanism solutions for events 1 to 3 (Table III). Open circles denote dilatations and solid circles compressions; *T* and *P* indicate axes of tension and compression.

plane striking N 80°W seems to be probable fault plane that dips at an angle of 40° in a direction N 10°E and the other nodal plane is dipping at an angle of 38° in south west direction. The quality of solution is fairly good. The maximum pressure axis appears to act in NNE-SSW direction. This is in good agreement with the thrust faults of the area (Krishnan 1966).

TABLE IV

Orientations of Nodal planes and T and P axes

(Azimuth and Plunge in degrees)

Event No.	1st Pole		2nd Pole		*T* axis		*P* axis	
	Az.	Pole	Az.	Pole	Az.	Plunge	Az.	Plunge
1.	14	17	271	38	229	12	329	41
2.	6	21	266	20	46	1	318	31
3.	60	38	196	40	124	64	216	1

DISTRIBUTION OF STRAIN IN TIME AND SPACE

Benioff (1949) has shown that the potential energy, J_p of a volume of rock W, possessing a coefficient of shear μ, strained by an average amount S immediately before an earthquake is given by

$$J_p = 0.5\ \mu\ WS^2 \qquad \ldots \qquad (10)$$

and the energy released as seismic waves by

$$J = 0.5\ \mu\ WS^2.f, \qquad \ldots \qquad (11)$$

where f is the fraction of energy released as seismic waves. In the present analysis, the value of strain S has been calculated from the magnitude energy relation of Gutenberg and Richter (1956) in the form

$$\log J = 11.8 + 1.5\ M, \qquad \ldots \qquad (12)$$

where M is the magnitude of an earthquake. The elastic strain rebound is proportional to the square root of the energy released, $\sqrt{J}$, which can be calculated from equation (12) by knowing the value of M.

(*a*) *Strain release in time :* Benioff (1949, 1951*a*, *b*) has investigated the strain release characteristics of various regions of the world including some after-shock sequences. In these studies Benioff has shown that the epicentres of the major earthquakes of the world lie on a great circle of the earth. Chouhan (1966, 1968) studied the strain release characteristics of the Indian regions. Chouhan *et al.* (1966) studied the seismicity of Assam and it was shown that the Sadiya and Dhubri regions are linked in such a way that only one region is active at a time.

The strain release map of the Delhi region including Kumaon has been prepared following Benioff's method using all the earthquakes of $M \geqslant 2$ since 1956. Cumulative strain release map (Fig. 6) shows that the amount of strain release started with a maximum in the year 1956. The release decreased gradually and became very small in the year 1962. From 1962 to 1966 the strain release was very small and by

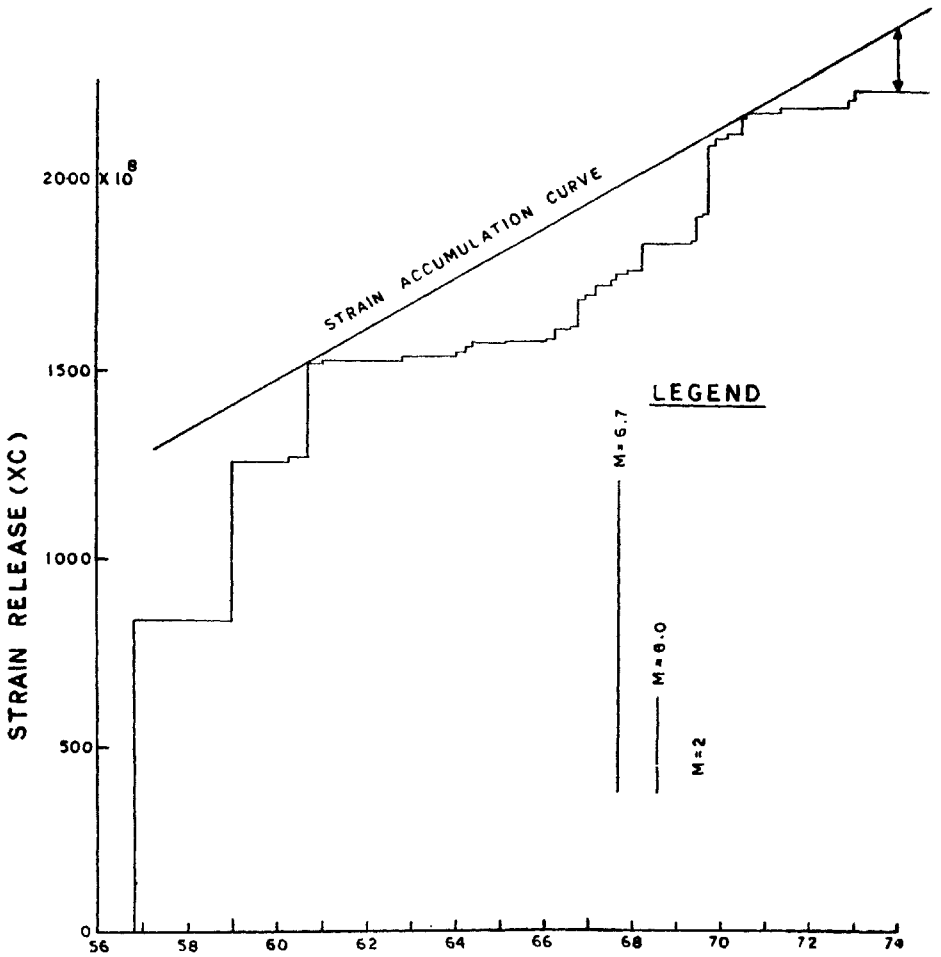

FIG. 6. Strain release characteristics of the Delhi region using M ≥ 2 from 1956 to 1972. Strain accumulation curve (linear) has been drawn slightly to the left of the zigzag curve and the arrow at the end of this curve shows the amount of accumulated strain.

the middle of 1966 to 1970 the strain release has been regular with fairly high value of release. Beyond 1970 the strain release has decreased.

Fig. 6 may be interpreted as, initially, there was huge accumulation of strain and this accumulation continued till 1956 when major part of it was released, resulting in the earthquake of 1956. Again in the year 1958 there was another major release which was followed by the third release in 1960, thus bringing the strain level to residual value. In this case the strain was released in instalments and had it been released in a single earthquake, the magnitude of the earthquake would have been 7. Since the strain release started in 1956, the period prior to 1956 may be termed as accumulation phase (quiescent period) and 1956 to 1960 as active period (release phases). From Fig. 6, it appears that the quiescent periods are followed by active

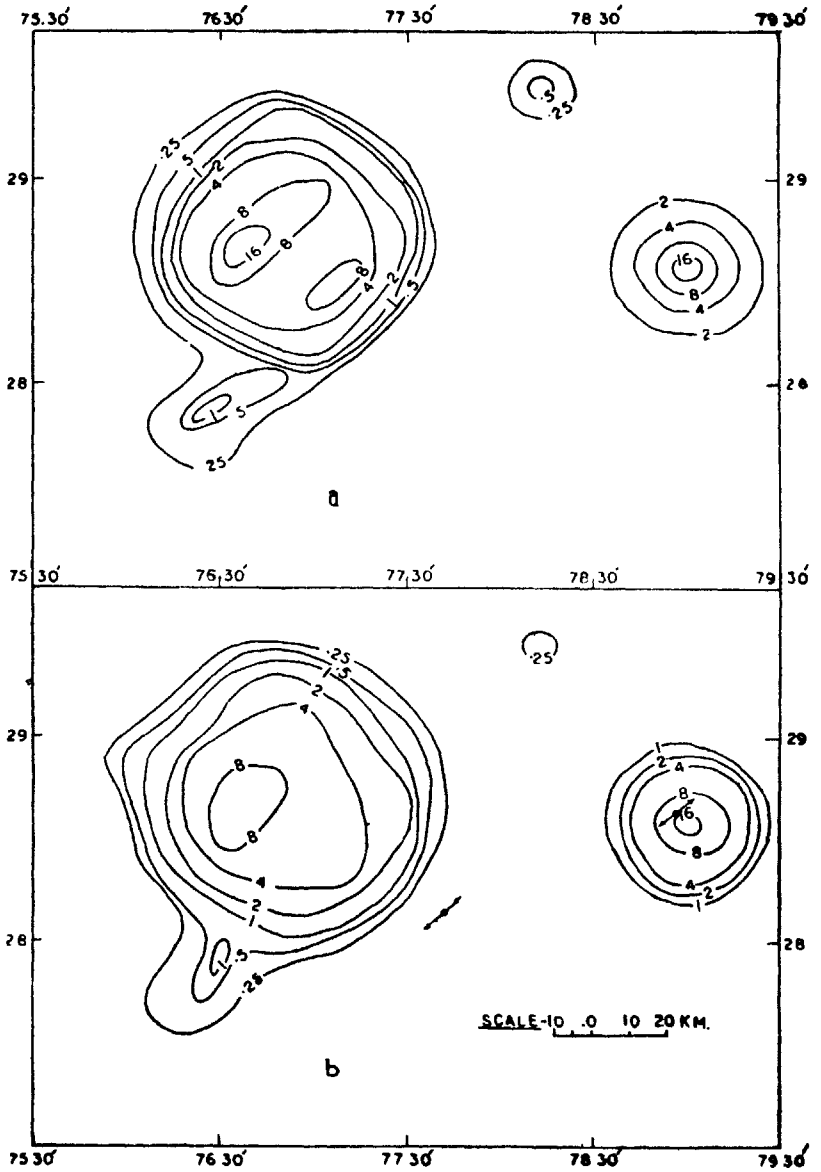

FIG. 7. Tectonic flux map of Delhi region using earthquakes from 1962 to 1972. First iteration is shown in Fig. a and second iteration in Fig. b. All the contour values are in the unit of 10^8 $(ergs)^{1/2}$.

period and the entire earthquake activity may be taken as representative of strain accumulation and relaxation. Thus, Fig. 6 shows strain accumulation curve (linear) from which the reserve of strain available to be released in future is shown by vertical line with arrows at the end. Following this concept, the maximum magnitude of an earthquake that may occur in Delhi in the near future is about 5.8.

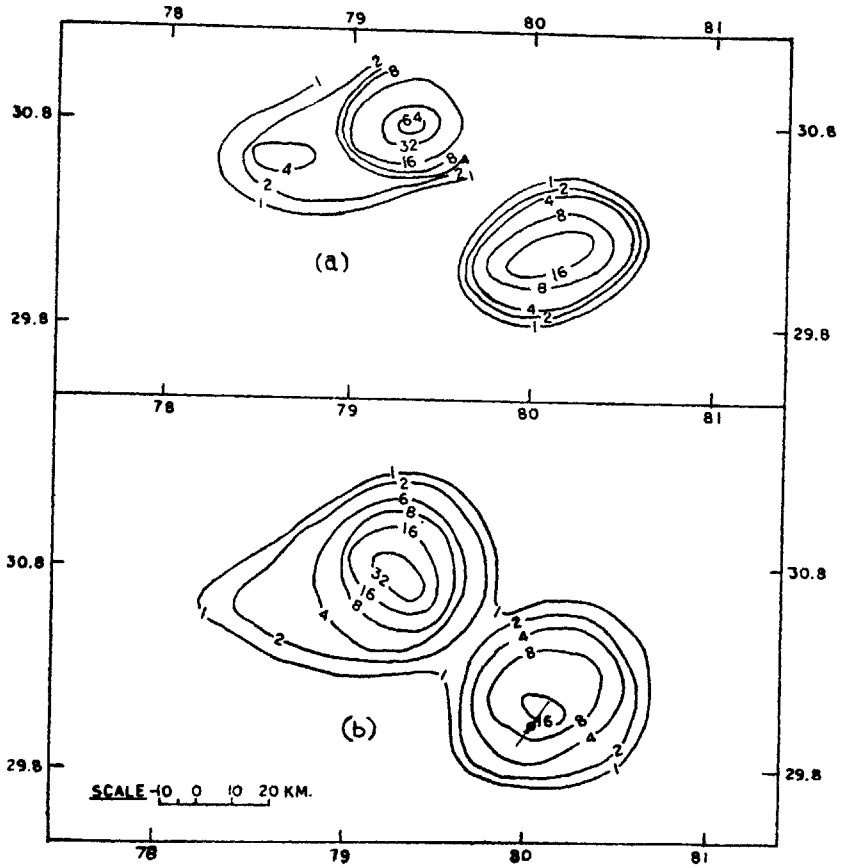

FIG. 8. Tectonic flux map of Kumaon Himalayas. All units and iterations are same as in Fig. 7.

(b) Strain release in space: Distribution of strain in space (tectonic strain) has been studied by S. Amand (1956), Bath (1956), Allen *et al.* (1965, 1966).

Following the method of Allen *et al.* (1965) and Chouhan (1968), the area around Delhi has been divided into squares of side 20 km and the strain released in each of these squares is plotted at the centres of each square for the Delhi and Kumaon regions. Then, the strain values at each of these squares are normalised to the adjacent squares in such a way that the bulk of strain (40 per cent of the strain) is distributed within the small area and the influence of the isolated large events is reduced (See Appendix II). This normalisation operation is known as iteration.

Fig. 7 shows smoothed tectonic flux contours of the Delhi region at contour intervals of .25, .5, 1 etc. in the unit of 10^8 (ergs)$\frac{1}{2}$ i.e., each preceding value is half of the following value. Fig. 7*a* is the first iteration and Fig. 7b is the second iteration. A glance at Fig. 7 suggests that the values of tectonic flux (strain in 7b) is distributed over a larger area and hence this method not only reduces the influence of isolated large events but also distributes the tectonic flux over a large volume of rocks,

Fig. 7a clearly demonstrates that if such a map is prepared for an isolated shock, it would result in circular contours without giving any additional information. This figure shows general trend of the active centres in the West of Delhi that strikes in the NE-SW direction. Second interation for this region (Fig. 7b) shows a general trend of active centres in a direction NNE-SSW (The tectonic trend already postulated by many geologists from field investigations). Moreover this trend of seismotectonics defines fairly well and supports the alignment of epicentral tracts in Sonepat area and at the same time it is quite unlikely that the trend continues up to Sonha. Similarly, the tectonic flux map, Fig. 8a, for the Kumaon region (iteration 1) shows no general trend but the second iteration (Fig. 8b) shows a clear trend of active tectonic zones with a general trend in the NW-SE direction.

Discussion

A transverse section of the Himalayas has been selected for the present study because it represents a tectonic Unit caused by geosynclinal loading (the Kumaon areas and the associated effect in the adjoining area, the Delhi region). In general under such loading the geosynclinal area is under compression and the adjoining area under tension. This has been clearly demonstrated from the three focal mechanism studies, where the direction of maximum tension and pressure axes remains same showing the continuation of same tectonic forces. Seismic activity associated with the Moradabad fault appear to be fairly deep seated as is evident from the offset distance of the two events (1 and 2) from the main fault (Fig. 1). However for the event 1 it may be due to error in the location of the epicentre also.

The most active seismic region appears to be the trijunction of Delhi-Hardwar ridge, Lahore-Delhi ridge and Axis of Delhi foldings. However the activity associated with the axis of Delhi folding appears to extend beyond Delhi towards the Himalayas. The area west of Delhi within a radius of 100 km. is an area of continuous seismicity (Richter 1971). Such areas are in general associated with complex faulting. The region east of Delhi seems to be an area of low incidence of earthquakes though the earthquakes may be of fairly high magnitude. This area is a region of sporadic seismicity. Such areas are in general associated with block faulting. Focal depths of shocks calculated are of the order of 8 km and since the nearest epicentral distance is about 10 km, the reliability of the determination is fairly high. In the light of the focal depth values it may be concluded that the origin of these shocks are of tectonic nature and thus supports Hukku's (1966) concept.

The regression curve shown in Fig. 4 shows that the ratio $a/b = 4.7$ which is the annual maximum magnitude that may occur in this area. This is an important measure of seismicity and it was shown by the author (1968) and Galanopaulos (1972) that, this is a measure to be used by earthquake engineers in the evaluation of earthquake rise. It is also claimed that this is the most reliable and stable measure of seismicity.

Conclusions

(1) The most active area in this region is the trijunction of the Lahore-Delhi ridge, Delhi-Hardwar ridge, and the Delhi axis of folding. The seismic activity of

the Delhi axis of folding appears to extend beyond Delhi. The focal depths of the shocks west of Delhi have been estimated to be about 8 km.

(2) Maximum magnitude of an earthquake that may occur once in a year appears to be 4.7 and the maximum size (magnitude) that may occur in this area is about 7.6.

(3) The focal mechanisms of earthquakes (events 1 and 2) of the Delhi area show tensional type of faulting with strike slip component to dip slip (normal component) in the ratio of 1.5:1, while the event No. 3 located in the Kumaon region shows a typical thrust faulting.

(4) From a consideration of strain accumulation and relaxation, it has been determined that the stored strain may precipitate in an earthquake of magnitude 5.8. The spatial distribution of strain for the Delhi and Kumaon regions shows seismotectonic trends of NNE-SSW and NW-SE directions respectively.

ACKNOWLEDGEMENTS

The author is grateful to Profs. V. K. Gaur, Jai Krishna and R. S. Mithal of Roorkee University for many suggestions from time to time. The author also thanks Prof. J. Singh for giving facility to carry out the present work and to I.M.D. for supplying the data.

Appendix I

Frequency-Magnitude Analysis and Seismic Activity

For groups of earthquakes whose magnitude distribution follows Gütenberg-Richter's law, the number of earthquakes N(M) with magnitude M and larger is given by

$$\log N(M) = a - bM = N_0\, 10^{-bm} = N_0\, e^{-b'm}$$

where $N_0 = N(O) = 10^{a}/b'$ and $b' = b \ln 10$

Hence it follows that $\log N(M) = a - bM - \log b'$

and $\log N(M) = b(M_1^* - M)$

where M_1^* is defined by $N(M_1^*) = 1$

or in general $N(M_i^*) = i$

or $bM_i^* = a - \log b' - \log i$

or $M_i^* = M_1^* - \log i/b$

Since $M_1^* = \left[\frac{a}{b} - \frac{\log b'}{b}\right]$

Thus a/b can be considered as an index of seismicity since $(\log b')/b$ is negligible (cf. Chouhan *et al.* 1968; Chouhan 1970; and Utsu 1971).

Appendix II

Method of Preparing Strain Release Map

Strain factors for each of the squares (20×20 sq. km) were computed for the period 1962-1972. The strain values, associated with shocks, have been plotted in the following manner.

(*i*) If the epicentre is located within the boundary of a square, the entire strain value is assigned to that square.

(*ii*) If the epicentre is located on a boundary, the strain is divided equally between the squares on either side.

(*iii*) If the epicentre is located at the intersection of the boundaries, then the strain value is divided equally to each of the four adjoining squares.

Thus the strain for each square is the sum of the strain values assigned to that area (square). Further smoothing was accomplished by a series of iterations, in each of which the strain release assigned to a given square was distributed and normalised as follows :—

40 per cent of the strain remains in the given square, 10 per cent is assigned to each of the four immediately adjoining squares and 5 per cent to each of the diagonally adjacent squares. Thus smoothed strain release maps are prepared applying any number of iterations as desired (cf. Allen *et al.* 1965; and Chouhan 1968).

References

Agocs, W. B. (1956). Report on Airborne magnetometer survey in Indo-Gangetic plains, India. *Rep. Min. nat. Resour. Scient. Res., Govt. of India (under Colombo Plan)—unpublished.*

Allen C. R. Amand, P. S., Richter, C. F., and Nordquist, J. M. (1966). Seismicity, Tectonism and surface faulting in the Western United States during historic times, *Bull. seis. Soc., Am.*, **56**, pp. 1105–1135.

Allen, C. R., Slemmons, D. B., and Gedney, L. D. (1965). Relationship between seismicity and geologic structure in southern California region. *Bull. seis. Soc. Am.*, **55**, pp. 753–797.

Amand, P. S. (1956). Two proposed measures of seismicity. *Bull. seis. Soc. Am.*, **46**, pp. 41–45.

Bath, M. (1956). A note on the measure of seismicity. *Bull. seis. Soc. Am.*, **46**, pp. 217–218.

Benioff, H. (1949). Seismic evidence for the fault origin of ocean deep. *Bull. geol. Soc. Am.*, **60**, pp. 1837–1848.

Benioff, H. (1951 *a*). Earthquakes and rock creep. *Bull. seis. Soc Am* , **41**, pp. 31–62.

Benioff, H. (1951 *b*). Global strain accumulation and release as revealed by great earthquakes. *Bull. geol. Soc. Am.*, **62**, pp. 331–338.

Bose, R. N. (1957). Report on refraction seismic investigations to locate the supposed sub-alluvial Delhi-Shahpur ridge, Punjab. *Rep., G.S.I.—unpublished.*

Chouhan, R. K. S. (1966). Regional strain release characteristics for Indian regions. *Bull. seis. Soc. Am.*, **56**, pp. 749-754.

———— (1968). Studies of seismicity of India and an analysis of some of strong earthquake sequences, Ph.D. thesis, Univ. Roorkee, *unpublished.*

———— (1970). On Frequency magnitude relation log $N = a - bM$. *J. pure appl. Geophys.*, **81**, pp. 119–123.

Chouhan, R. K. S., Gaur, V. K., and Mihal, R. S. (1966). Seismicity of Assam. *Third Symp. Earthq. Engn. Roorkee*, U.O.R., November 1966, pp. 423–430.

Drakopoulos, J. C., and Srivastava, H. N. (1972). The dependence of earthquake frequency magnitude relationship and strain energy release upon the focal depth in Hindu-kush region. *Ann. di Geofis.*, **25**, pp 593–606.

Galanopoulos, A. G. (1972). Face to face with the elements rage. *Ann. Geol. des Pays Helleniques*, **24**, pp. 462–466.

Ghosh, A. M. N. (1959). Review of the possible oil bearing sedimentary basins. M.R.D. series no. 10 (U. N. Publication).

Gütenberg, B., and Richter, C. F. (1954). *Seismicity of the Earth and associated phenomena.* Princeton University Press.

———— (1956). Magnitudes and energy of earthquakes. *Ann. di Geofis.*, **9**, pp. 1–15.

Hodgson, J. H., and Storey, R. S. (1953). Tables extending Byerly's fault plane technique to earthquake of any focal depth. *Bull. seis. Soc. Am.*, **43**, pp. 49–61.

Hukku, B. M. (1964). Report on the Geological investigations of the minor earthquakes around Sonepat, Punjab, G.S.I.—*Unpublished*

———— (1966). Probable causes of earthquakes in the Delhi-Sonepat area. Third Symposium, Earthq. Engng., Roorkee, U.O.R., Nov. 1966, Part II, pp. 75–80.

Isacks, B., and Oliver, J. (1964). Seismic waves with frequencies from 1 to 1000 cycles per second recorded in a deep mine in northern, New Jersey. *Bull. seis. Soc. Am.*, **54**, pp. 1941–1979.

Jhingran, A. G., and Puri, S. N. (1963). Seismicity of the Delhi region with reference to the Himalayas. *Symp. Himalayan Geology, Calcutta*, October, 1963.

Krishnan, M. S. (1966). Tectonics of India. *Symp. Tectonics, Natn. Inst. Sci. India*, pp. 1–36.

Krishnaswamy, V. S. (1962). Significance of the Moradabad fault in the Indo-Gangetic Basin and other faults in the sub-Himalayas in relation to the Ramaganga River Project, U.P. *Proc. 2nd Symp. Earthq. Engng.*, Roorkee, U.O.R. 1962, pp. 411-422.

Muktinath, Kedarnarain and Srivastava, J.P. (1960). A report on the Delhi earthquake of 27th August 1960. *Rep. GSI, —unpublished.*

Negi, B. S., and Eremenko, N. A. (1968). Tectonic map of India. ONGC, Dehradun (India).

Page, R. (1968). Aftershocks and microaftershocks of the great Alaska earthquake of 1964. *Bull. seis. Soc. Am.*, **58**, pp. 1131–1168.

Richter, C. F. (1971). Sporadic and continuous seismicity of Faults and regions, recent crustal movements. *Bull. R. Soc. N. Zealand*, **9**, pp. 171–173.

Ritsema, A. R. (1955). The fault plane technique and the mechanism in the focus of Hindukush earthquakes. *Indian J. Met. Geophys.*, **6**, pp. 1–10.

Sharma, S. (1965). Report on the investigations into probable causes of earthquakes, tremors near Sonepat, Punjab—*Unpublished.*

Simha, K. R. Madhwa (1959). Report on refraction seismic investigations to locate the supposed sub-alluvial Delhi-Shahpur ridge Punjab. *Rep., G.S.I.—Unpublished.*

Singh, Mohinder (1964). *The Tribune*, October 15.

Srivastava, L. S., and Somayajulu, J. G. (1966). The seismicity of the area around Delhi. Third Symp. earthq. Engng. Roorkee, U.O.R., 1966, pp. 417–422.

Sykes, Lynn. R. (1967). Mechanism of earthquakes and nature of faulting on the Mid-oceanic ridges *J. geophys. Res.*, **72**, pp. 2131–2153.

Tandon, A. N., and Choudhury, H. M. (1966). A report on the seismicity studies by the India Meteorological Department. *Third Symp. Earthq. Engng. Roorkee*, U.O.R. 1966, Part II, pp. 34–43.

Tocher, D. (1959). Seismographic results from the 1957, San Francisco Earthquakes. *Calif. Div. Mines, Spec. report* **57**, pp. 60–73.

Utsu, T. (1965). A method for determining the value of *b* in a formula Log N = *a* —*bm* showing the magnitude frequency relation for earthquakes. *Geophys. Bull. Hokkaido Univ.*, **13**, pp. 99–104.

———— (1967). Some Problems of the frequency distribution of earthquakes in respect of magnitude, *Geophys. Bull Hokkaido Univ.*, **17**, pp. 53–59.

———— (1971). Aftershocks and earthquake statistics III. *J. Fac. Sci. Hokkaido Univ.*, Series IV, **3**, pp. 379–441.